Oscillating Gadolinium thermal switch

N PETELIN[(a)], B PEČAR[(b)], D VRTAČNIK[(b)], J PERNE[(a)], U TOMC[(a)], A KITANOVSKI[(a)]*

[(a)] University of Ljubljana, Faculty of Mechanical Engineering
Ljubljana, 1000, Slovenia, andrej.kitanovski@fs.uni-lj.si
[(b)] University of Ljubljana, Faculty of Electrical Engineering
Ljubljana, 1000, Slovenia, danilo.vrtacnik@fe.uni-lj.si

ABSTRACT

Thermal control devices such as thermal switches, thermal diodes and thermal regulators are two-terminal devices used to passively or actively control the intensity and direction of heat flow, which has proven useful in various thermal management applications, including caloric technologies. Here, a millimetre-scale oscillating gadolinium thermal switch is constructed using commercially available materials, with steady-state switching ratio of r_{switch} = 2,3. The thermal switch uses electrostatic forces for actuation and makes thermal contact between the heat source and the heat sink when in the ON state, and breaks contact when in the OFF state. In the ON state when the thermal switch is oscillating the Gd plate transfers heat, while in the OFF state, the Gd plate does not oscillate and heat is transferred via parasitic conduction through air gap and device's housing. The thermal conductance is $2{,}42 \cdot 10^{-1}$ W/K in the ON state and $1{,}22 \cdot 10^{-1}$ W/K in the OFF state. The thermal switch exhibits consistent and repeatable actuation over more than > 10^5 oscillation cycles and can be used to actively route heat flows in thermal management applications. Our proof-of-concept device has a convenient geometry and can be easily implemented in various thermal management system where implementation and/or operation of conventional thermal management methods are not suitable.

Keywords: thermal control elements, thermal switch, thermal management, magnetocaloric cooling/heating.

1. INTRODUCTION

Efficient thermal management is crucial for improving energy efficiency and ensuring optimal performance, reliability and safety of systems. Conventional thermal management methods such as large-scale heat exchangers, thermal resistors and thermal capacitors struggle to meet the requirements of modern, particularly compact systems with high power density and varying temperature gradients. In response to these challenges, a new concept of thermal control devices has emerged that includes thermal switches, diodes and capacitors. These devices provide non-linear, switchable and active heat control, similar to the way their electrical counterparts control electric current, and are suitable for a wide range of sizes, from sub-micrometre to larger systems of over 100 mm.

Thermal switches are active thermal devices in which the steady-state thermal conductance denoted as $G = Q/\Delta T$, can be toggled between an ON and an OFF state [1,2]. Ideally, the thermal conductance is infinitely high in the ON state and zero in the OFF state. A figure of merit for a thermal switch is the switching ratio r between the highest archived thermal conductance G_{on} (the ON state) and the lowest achievable thermal conductance G_{off} (the OFF state). Thermal control devices can be used in a wide range of applications, from solid-state cooling [3–7] to thermal regulation of buildings [8,9], electronics, batteries[10,11] and solar thermal energy storage [12,13].

Similar to their electrical counterparts, thermal switches rely on a non-thermal control parameter, such as electric fields, magnetic fields, or pressure, to modulate thermal conductance. The devices with the highest thermal switching ratio utilise electrostatic actuation to make and break thermal contacts between hot and cold spots [3,14–16]. Electrostatic actuation is characterized by its compactness, quiet operation and energy efficiency [17]. However, unlike magnetic actuation [18–21] or external electromotor-driven actuation, which offer larger actuation strokes [7,22–25], it requires precise engineering to achieve small contact gaps between hot and cold spots.

In this study, we present an electrostatic millimetre-scale oscillating thermal switch that can be used to influence the heat flow between the hot spot and the heat sink. First, the performance of the device is predicted theoretically using the online simulation tool TCC builder. Later, we experimentally investigated the behavior and switching ratio of the thermal switch under different conditions and demonstrated its ability to actively control the heat flux in low power density applications at room temperature.

1.1 Thermal switch concept

The main part of the device consists of an oscillating 161 µm thick Gd plate (Heeger Materials) and two Si plates (MicroChemicals GmbH) with a thickness of 516 um, which serve as hot and cold heat exchangers. The Gd plate was polished to create an optically reflective surface and to reduce the thermal contact resistance associated with surface asperities. The gold electrode was sputtered onto the Gd surface, while the graphite electrodes (Chemie Graphit 33) were spray-coated onto the heat exchangers. A 32 µm thick polyamide film (CAPLINQ, PIT0.5S) with a one-sided silicone adhesive (16 µm polyamide, 16 µm silicone adhesive) was attached to the graphite electrode, creating a structure of Si/graphite layer/ polyamide film on the side of the hot heat exchanger (HHEX). The same structure was also applied to the cold heat exchanger (CHEX). The polyamide film prevents a short circuit when the Gd plate moves between the cold and hot heat exchanger. The Si wafer with the corresponding layers is inserted into a housing printed with a 3D printer, which serves as a spacer. The thickness of the air gap is 310 µm. The Gd plate is freely movable and not attached to the spacer structure. To reduce heat loss through the spacers, the housing is printed from a material with low thermal conductivity. The total mass of the device with housing is 10.31 g, the mass of the thermal switch is 2.18 g. The electrodes were connected to an amplifier (TREK 2220) using thin copper wires. In order to generate a time-varying voltage at the electrodes, the voltage signal at the rectifier (Dr.meter PS-3010DF) was controlled by an Arduino (Uno) control system. According to the control signal, the Gd plate oscillated between the cold and hot heat exchanger. The size of cold and hot heat exchangers is 55.11 mm × 40.11 mm, but the active area is smaller, measuring 34.8 mm × 53 mm. This area corresponds to the size of the Gd plate, which serves as a thermal switch in our case. Figure 1 shows a cross-section of the device with the positions of the thermocouples marked in purple. The entire housing of the device was insulated with 30 mm thick thermal insulation (Armaflex) to reduce heat loss to the surroundings (not shown in figure 1). The heat source was simulated by a flexible electric thin-film heater (KLC, 8.17 W). The electric heater was attached to the hot heat exchanger on one side and insulated with thermal insulation (Armaflex) on the other side. By adjusting the electrical power of the electric heater, different temperatures were generated on the surface of the hot heat exchanger.

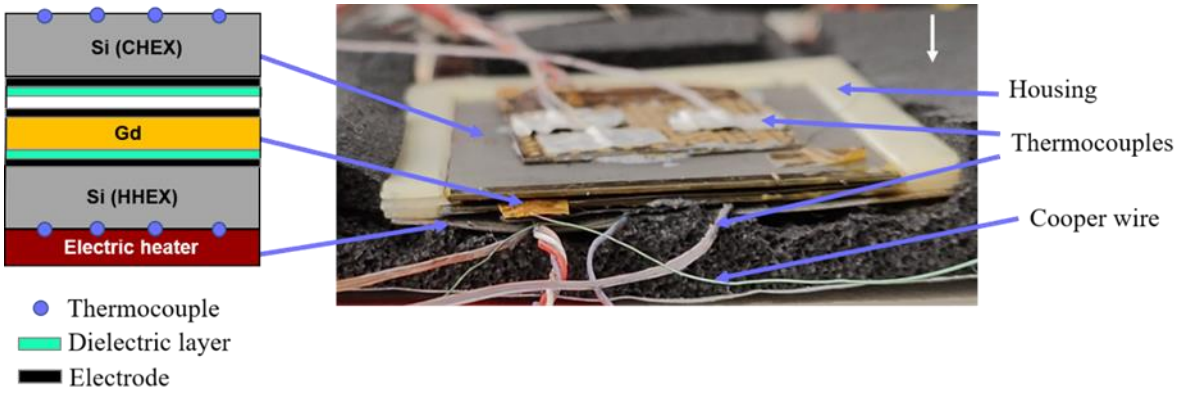

Figure 1: Cross section of the thermal switch device.

2. TCC BUILDER

First, we evaluated the performance of the device with the TCC builder. The TCC builder is an online tool for designing thermal control elements and thermal control circuits with a user-friendly interface and an associated library of materials and thermal control elements. A schematic representation of the device in TCC builder is shown in Figure 2 and consists of six main components: Hot Heat Exchanger (HHEX), Polyamide, air, Gd, Polyamide and Cold Heat Exchanger (CHEX). The Gd and air change position according to the operating frequency that dictate the heat transfer time. The electrodes are not included in the simulations as they are only a few nanometers thick and are also made of highly conductive material. The

selected boundary conditions were: Heat input on the HHEX side, which represents the electrical power of the electric heater, and on the CHEX side the adiabatic wall was chosen as boundary condition. The power density of the electric heater was 95 W/m^2. The thermal switch is ON, with high thermal conductance G_{on}, when it is in contact with the cold heat exchanger, and is OFF with low thermal conductance G_{off} when it is in contact with the hot heat exchanger. The thermal conductance in the ON state G_{on} is primarily affected by the thermal contact resistance between Gd and the Si heat exchangers. Thermal contact resistance depends mainly on the contact pressure, the surface roughness, the ambient pressure (air pockets trapped between the surface asperities) and the choice of materials in contact (presence or absence of thermal interface materials). In addition to the factors mentioned above, convection heat losses at higher operating frequencies also have a significant influence on G_{on} [166]. In the OFF state, the thermal conductance G_{off} is affected by the heat conduction through the housing of the spacer $G_{housing}$, the heat conduction through the air gap G_{air} and the heat transfer by radiation G_{rad} between Gd and the polyamide film. The Gd moves between HHEX and CHEX with an operating frequency of 0.25 Hz, where the time for each heat transfer process is 2 s and the time for the Gd position change is 6.25 ms, which was determined experimentally. The thermal contact resistance between Si and polyamide in contact was 8.4 m²K/W and between Gd and polyamide was 9.1 m²K/W. These values were taken from reference [26]. In the TCC builder, the user can switch between different scales in the program, which determine how much real length can be placed on the TCC-Builder canvas. We have chosen a scale of 100 um so that a 10 mm thermal control circuit fits on the canvas. If the thickness of one of the elements of the thermal control circuit is too large or too small to fit on the canvas, the thickness and therefore the effective thermal conductivity must be changed, as the thermal resistance must remain unchanged. This applies if the thermal mass of the element does not significantly affect the operation of the device. Therefore, the polyamide with a thickness of 32 µm was instead modelled with a thickness of 100 µm to fit the circuit on the canvas. For this reason, the thermal conductivity of the polyamide was changed from 1.25 W/mK to 3.906 W/mK. Since the Gd oscillates between HHEX and CHEX due to electrostatic forces, Joule heating is also included in the simulation as volumetric heat gain. The current and voltage for the electrostatic actuation were 0,1 mA and 800 V. The results show that the thermal conductance is 1.05 W/K when the thermal switch is on and 0.428 W/K when it is off. The corresponding switching ratio r is 2.5.

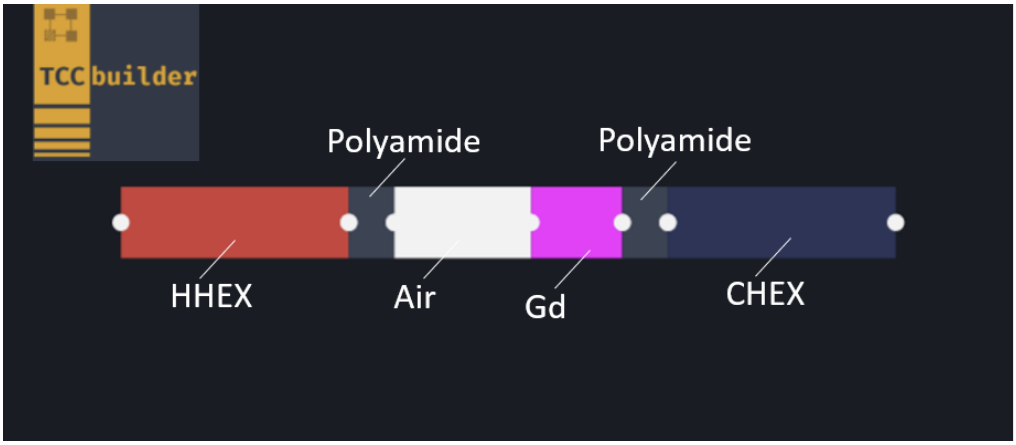

Figure 1: Device with thermal switch as presented in TCC builder.

3. EXPERIMENTAL RESULTS

Figure 2 shows the experimentally determined thermal conductance of the thermal switch in the ON (blue colour) and OFF state (black colour) as a function of the power of the electric heater. In the OFF state, the thermal switch has a low thermal conductance G_{off}, which ranges from 0,8 $\cdot 10^{-1}$W/K to 1,7$\cdot 10^{-1}$ W/K. In the ON state, however, the thermal conductance G_{on} is higher and reaches values of 1,2$\cdot 10^{-1}$ W/K to 4,0$\cdot 10^{-1}$ W/K at an operating frequency of 0.5 Hz.

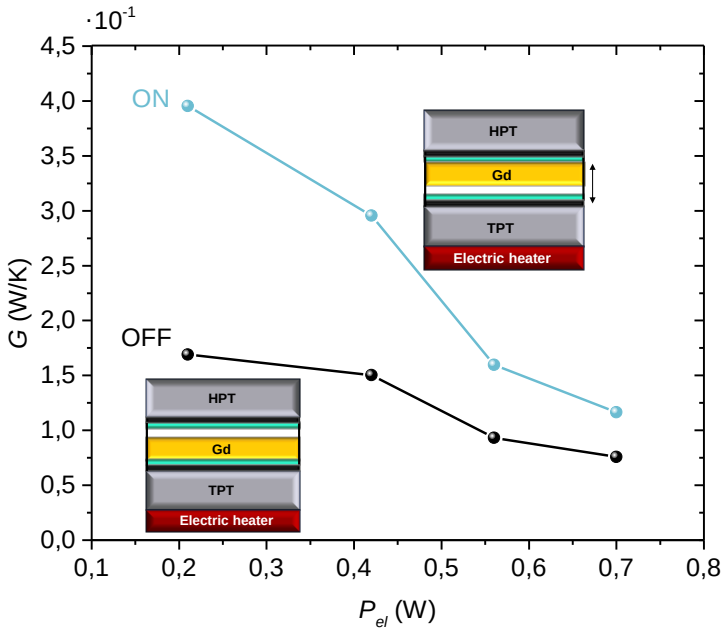

Figure 2: Thermal conductance G in ON and OFF state at different electrical power P_{el}.

The switching ratio is defined as $r_{switch} = G_{on} / G_{off}$ and is the primary metrics for evaluating thermal switch performance. Measurements were made at four different heating powers: 0.7 W, 0.56 W, 0.42 W and 0.21 W. As the heating area has a size of 55.11 mm × 40.11 mm, these values correspond to 316.7 W/m^2, 253.3 W/m^2,190 W/m^2, 95 W/m^2.

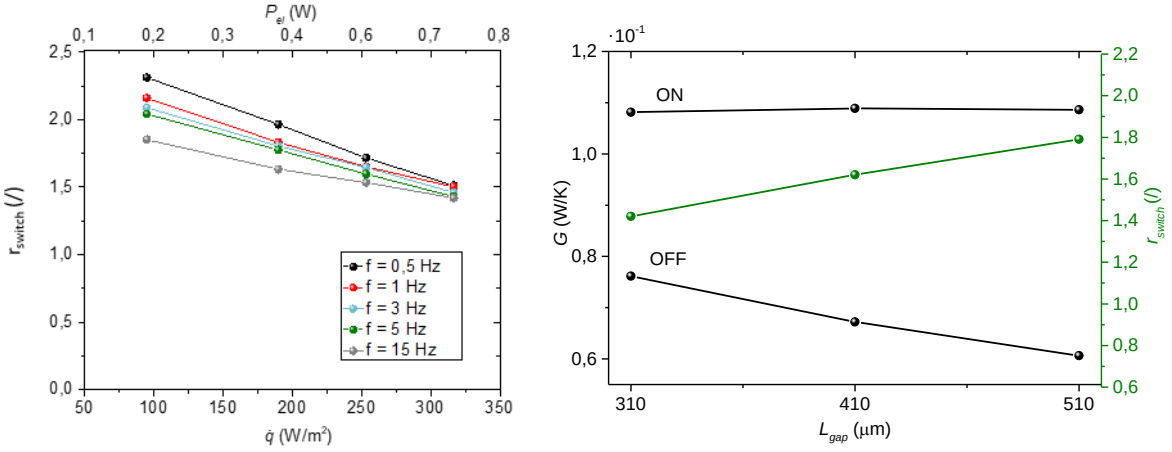

Figure 3: (a) Switching ratio r_{switch} as a function of the operating frequency and the electrical power of the electric heater P_{el}. (b) Different air gap sizes and their influence on the thermal conduction of the thermal switch.

Figure 3(a) shows that the maximum switching ratio r_{switch}= 2.3 achieved was at an operating frequency of 0.5 Hz and a minimum heating power of 0.21 W. As the frequency increases, the convection losses that occur during the movement of the Gd plate increase, which is particularly noticeable at low operating powers. The convection losses could be reduced by closing the entire device with a thermal switch and thus preventing the exchange with the surrounding (colder) air. Figure 3 (b) shows the influence of the air gap size on the thermal conductance when switched ON and OFF at an operating frequency of 15 Hz. The measurements were carried out with three different air gap sizes: 310 µm, 410 µm, 510 µm, with a heating power of 0.7 W. As the air gap increases, the thermal conductance G_{off} decreases in the OFF state, while the air gap size in the ON state does not significantly affect the thermal conductance G_{on}. By increasing the air gap size, the switching ratio also increases, as the OFF state the device has better thermal insulation properties. Increasing the air gap from 310 µm to 510 µm increased the switching ratio by 26%, from r_{switch} =

1.4 to r_{switch} = 1.8. It should be noted that the electrostatic field decreases as the air gap increases, which plays an important role in operation if the air gap is increased further. If the device were in a vacuum, heat transfer by conduction through the air gap would not occur and the only heat transfer mechanism in the OFF state would be heat conduction through the housing and heat transfer by radiation. This would increase the switching ratio as the thermal conductivity in the OFF state G_{off} would be significantly lower. In a similar design using magnetic forces for actuation, the switching ratio increased from 2,1 in air to 34 in vacuum [27]. In addition, the thermal contact resistance is lower in vacuum than in air, as the air trapped in the irregularities on the surface acts as a thermal insulator and reduces the transferred heat flux [28]. Heat transfer by radiation plays only a minor role, as the temperature difference between the hot and cold heat exchanger is relatively small (< 6 K). If we compare the result from 1D numerical simulation in TCC builder for 310 μm air gap and 95 W/m^2 heating power, we can see that in the ON state the experimentally determined thermal conductance is $G_{on,exp}$ = 0.108 W/K, while the numerical predicted thermal conductance is 10 times higher and is $G_{on,num}$ = 1.05 W/K. One of the main reasons are the heat losses to the environment, which were not considered in the numerical model, and the second reason is that in the experimental setup the thermocouples on the surfaces create small bumps that increase the thermal contact resistance when Gd oscillates between the hot and cold heat exchanger. In the OFF state, the experimental thermal conductance value is $G_{off,exp}$ = 0.077 W/K, while the numerically predicted value is 5 times higher and is $G_{off,num}$ = 0.428 W/K.

During the OFF state in the numerical simulations, heat gains from the electric heater to the cold heat exchanger occur only through heat conduction within the air gap. Conversely, in the experimental set-up heat gains extend towards the ambient surroundings, consequently resulting in a reduced amount of heat leakage towards the cold heat exchanger. Therefore, the experimentally determined switching ratio is $r_{switch,exp}$ = 1.4 and the numerical determined switching ratio is $r_{switch,num}$ = *2.5.*

4. CONCLUSIONS

In summary, we have numerically simulated in experimentally demonstrated a millimetre-scale thermal switch that uses electrostatic forces to make and break thermal contact between the Gd surface and the heat exchangers. Our experimental results show that the switching ratio is r_{switch}= 2.3 at a heating power of 95 W/m^2 (0.21 W). The thermal switch has a rigid stationary frame that could be enclosed, which would reduce convection losses and also allow operation in a vacuum. Operating in a vacuum would reduce heat conduction through the air gap in the OFF state, which could significantly improve the switching ratio. Another way to improve the switching ratio would be to increase the electric field between the electrodes, which would reduce the thermal contact resistance between the thermal switch and the heat exchanger. This could be achieved simply by increasing the voltage amplitude, but the maximum voltage for the same dielectric layer thickness is limited by the dielectric strength of the chosen material and its ability to withstand a voltage before breakdown occurs. The device is constructed using commercially available materials and can be easily incorporated into existing devices that operate at room temperature. The thermal switch has demonstrated consistent and repeatable actuation over more than 500 thermal cycles.

ACKNOWLEDGEMENTS

The authors acknowledge the financial support of the Slovenian Research Agency for the projects TCCbuilder: An open-source simulation tool for thermal control circuits J7-3148, MagBoost: Magnetocaloric booster micro-heat pump for district heating system L2-2610, MHD-magcool: Novel MHD-thermal switch essential for nonconventional magnetic cooling system BI-DE/21- 22-008, and the research core funding no. P2-0223. This work was also financially supported by the Slovenian Research Agency as part of the Young Researcher PhD program.

REFERENCES

[1] Wehmeyer G, Yabuki T, Monachon C, Wu J and Dames C 2017 Thermal diodes, regulators, and switches: Physical mechanisms and potential applications *Appl. Phys. Rev.* **4**

[2] Klinar K and Kitanovski A 2020 Thermal control elements for caloric energy conversion *Renew. Sustain. Energy Rev.* **118**

[3] Ma R, Zhang Z, Tong K, Huber D, Kornbluh R, Ju Y S and Pei Q 2017 Highly efficient electrocaloric cooling with electrostatic actuation *Science (80-.).* **357** 1130–4

[4] Bo Y, Zhang Q, Cui H, Wang M, Zhang C, He W, Fan X, Lv Y, Fu X, Liang J, Huang Y, Ma R and Chen Y 2021 Electrostatic Actuating Double-Unit Electrocaloric Cooling Device with High Efficiency *Adv. Energy Mater.* **11** 1–8

[5] Bradeško A, Fulanović L, Vrabelj M, Matavž A, Otoničar M, Koruza J, Malič B and Rojac T 2021 Multifunctional Cantilevers as Working Elements in Solid-State Cooling Devices *Actuators* **10**

[6] Meng Y, Zhang Z, Wu H, Wu R, Wu J, Wang H and Pei Q 2020 A cascade electrocaloric cooling device for large temperature lift *Nat. Energy* **5** 996–1002

[7] Wang Y, Schwartz D E, Smullin S J, Wang Q and Sheridan M J 2017 Silicon Heat Switches for Electrocaloric Cooling *J. Microelectromechanical Syst.* **26** 580–7

[8] Varga S, Oliveira A C and Afonso C F 2002 Characterisation of thermal diode panels for use in the cooling season in buildings *Energy Build.* **34**

[9] Booten C, Rao P, Rapp V, Jackson R and Prasher R 2021 Theoretical Minimum Thermal Load in Buildings *Joule* **5**

[10] Hao M, Li J, Park S, Moura S and Dames C 2018 Efficient thermal management of Li-ion batteries with a passive interfacial thermal regulator based on a shape memory alloy *Nat. Energy* **3** 899–906

[11] Zeng Y, Zhang B, Fu Y, Shen F, Zheng Q, Chalise D, Miao R, Kaur S, Lubner S D, Tucker M C, Battaglia V, Dames C and Prasher R S 2023 Extreme fast charging of commercial Li-ion batteries via combined thermal switching and self-heating approaches *Nat. Commun.* **14**

[12] Muhumuza R, Zacharopoulos A, Mondol J D, Smyth M and Pugsley A 2019 Experimental study of heat retention performance of thermal diode Integrated Collector Storage Solar Water Heater (ICSSWH) configurations *Sustain. Energy Technol. Assessments* **34**

[13] Pugsley A, Zacharopoulos A, Deb Mondol J and Smyth M 2019 Theoretical and experimental analysis of a horizontal planar Liquid-Vapour Thermal Diode (PLVTD) *Int. J. Heat Mass Transf.* **144**

[14] Jahromi A E and Sullivan D F 2014 A piezoelectric cryogenic heat switch *Rev. Sci. Instrum.* **85** 85–8

[15] Keum H, Seong M, Sinha S, Kim S, Keum H, Seong M, Sinha S and Kim S 2012 Electrostatically driven collapsible Au thin films assembled using transfer printing for thermal switching *Appl. Phys. Lett.* **100**

[16] Beasley M A, Firebaugh S L, Edwards R L, Keeney A C and Osiander R 2004 MEMS Thermal Switch for Spacecraft Thermal Control *Proc. SPIE 5344, MEMS/MOEMS Components and Their Applications* vol 5344 p 4

[17] Meng Y, Zhang Z, Wu H, Wu R, Wu J, Wang H and Pei Q 2020 A cascade electrocaloric cooling device for large temperature lift *Nat. Energy* **5** 996–1002

[18] Ahmim S, Almanza M, Pasko A, Mazaleyrat F and Lobue M 2018 Study of the energy conversion chain in a thermomagnetic generator *Thermag VIII, Darmstadt, Ger.* 197–201

[19] Bulgrin K E, Lavine A S and Ju Y S 2009 Magnetomechanical thermal diode with tunable switching *Mater. Sci.*

[20] Chong Tai Y and Wright J A 2001 Fabrication and using a micromachined magnetostatic relay or switch, Patent US 6320145 B1

[21] Tai C Y, Wong Y, Rodenbush A J, Joshi C H and Shirron P J 2010 A High Conductance Detachable Heat Switch for ADRs *AIP Conf. Proc.* **710** 443–50

[22] Smullin S J, Wang Y and Schwartz D E 2015 System optimization of a heat-switch-based electrocaloric heat pump *Appl. Phys. Lett.* **107**

[23] Ossmer H, Miyazaki S and Kohl M 2015 Elastocaloric heat pumping using a shape memory alloy foil device *Transducers* pp 726–9

[24] Ossmer H, Wendler F, Gueltig M and Lambrecht F 2016 Energy-efficient miniature-scale heat pumping based on shape memory alloys *Smart Mater. Struct.* **25**

[25] McCarty R 2007 Experimental Verification of Thermal Switch Effectiveness in Thermoelectric Energy Harvesting *J. Thermophys. Heat Transf.* **21**

[26] Petelin N, Kalin M and Kitanovski A 2023 A conceptual design of a thermal switch capacitor in a magnetocaloric device: experimental characterization of properties and simulations of operating characteristics *JPhys Energy* **5**

[27] Castelli L, Garg A, Zhu Q, Sashital P, Shimokusu T J and Wehmeyer G 2023 A thermal regulator using passive all-magnetic actuation *Cell Reports Phys. Sci.* **4**

[28] Madhusudana C V 2014 *Thermal Contact Conductanc,* (New York: Springer) 25-77